MULTIPHYSICS MODELLING OF BIOMASS AND PLASTICS WASTE CO-PYROLYSIS

OLAYIWOLA, R. O.[1,2*], OLAYIWOLA, F. T.[3], AUDU, A. O.[4], YUSUF, Y.[5], IBRAHIM, M.[5], & IBRAHIM, J. A.[5]

[1]Department of Mathematics and Statistics,
Confluence University of Science and Technology, Osara, Nigeria.
[2]Department of Mathematics, Federal University of Technology, Minna, Nigeria.
[3]Department of Computer Science, Federal University of Technology, Minna, Nigeria.
[4]Department of Mathematics, Federal University of Education, Kontagora, Nigeria.
[5]Department of Mathematical Sciences, Ibrahim Badamasi Babangida University, Lapai, Niger State, Nigeria.
E-mail.: olayiwolaro@custech.edu.ng

Abstract
Co-pyrolysis of biomass and plastic waste is an innovative and promising approach for converting these materials into valuable products such as bio-oil, syngas, and biochar. This process is gaining attention for its ability to manage plastic waste and biomass while producing energy-rich outputs. In this study, two modelling approaches were used to investigate the energy-related synergistic effect between polystyrene (PS) and bamboo waste. The problem is formulated in terms of non-linear partial differential equations. Approximate solutions for the non-linear energy equation are obtained by using Olayiwola's generalised polynomial approximation method (OGPAM). To obtain a clear insight into the physical problem, the temperature behaviours are discussed for different dimensionless parameters involved in the governing equations. Graphical representations and discussions are also presented. The results show that both modelling approaches give an appreciable synergy effect of reduction in overall energy when PS and bamboo are co-pyrolysed together. However, the second approach, which allows interaction between the two feedstocks, gives a greater reduction in overall energy usage up to 79%, depending on the ratio of PS in the mixed blend.

Keywords: Arrhenius kinetics, biomass, co-pyrolysis, OGPAM, plastics waste, pyrolysis.
[2010] Mathematics Subject Classification: 80A25, 76S05

Introduction
Pyrolysis is a thermochemical decomposition process that converts organic materials into biofuels and valuable by-products in the absence of oxygen. While biomass pyrolysis results in highly oxygenated bio-oil, plastic pyrolysis predominantly produces hydrocarbon-rich compounds. Co-pyrolysis combines these two feedstocks to enhance bio-oil quality and improve energy recovery (Sharma *et al.*, 2021).

The co-pyrolysis of biomass and plastic waste has gained significant attention as a sustainable method for converting waste into valuable energy products such as bio-oil, syngas, and char. Several studies have demonstrated that the co-pyrolysis of biomass and plastics reduces oxygenated compounds and increases the production of long-chain hydrocarbons (Wang *et al.*, 2020). This synergistic effect is attributed to hydrogen transfer reactions, where plastics act as a hydrogen donor, improving the stability of bio-oil. Wang *et al.* (2020) found that blending polypropylene (PP) with lignocellulosic biomass led to an increase in aromatic hydrocarbons and reduced acidic components in bio-oil. Li *et al.* (2019) observed that co-pyrolysis of pine sawdust with polyethene (PE) resulted in a 30% improvement in energy recovery efficiency compared to individual pyrolysis.
Computational analysis of co-pyrolysis involves the use of kinetic modelling, machine learning, and computational fluid dynamics (CFD) to predict product distribution and optimise process conditions.

Kinetic modelling helps describe the thermal decomposition of biomass and plastics through different reaction pathways. Common kinetic models include Arrhenius-Based Models. These models use activation energy and reaction rate constants to predict decomposition behaviour (Xie *et al.*, 2021). Other kinetic models include the Distributed Activation Energy Model (DAEM). This model accounts for multiple reaction pathways, providing a more accurate representation of pyrolysis (Zhang *et al.*, 2019).

Recent studies have explored machine learning (ML) techniques such as artificial neural networks (ANN) and support vector machines (SVM) to improve pyrolysis predictions (Gao *et al.*, 2022). CFD simulations provide insights into heat transfer, fluid flow, and chemical reactions in pyrolysis reactors. Studies by Singh *et al.* (2020) demonstrated that CFD modelling could optimise reactor temperature profiles and gas residence time, improving process efficiency.

Despite extensive biomass and plastic pyrolysis research, limited studies have comprehensively modelled the thermochemical interactions in co-pyrolysis systems. There are critical gaps in understanding how biomass-plastic interactions modify product formation pathways and in developing integrated models that couple reaction kinetics, heat transfer, and mass transfer for co-pyrolysis.

This study addresses these gaps by developing a comprehensive mathematical model and computational framework for biomass-plastic waste co-pyrolysis. The model will predict the overall energy synergistic effect that may exist in the co-pyrolysis of bamboo and polystyrene.

Materials and Methods

Problem Formulation

In this approach, the pyrolysis model was developed to model the interaction between the two feedstocks, Biomass (Bamboo) and Plastics (Polystyrene), at the same time, at a pre-defined ratio as shown in Figure 1.

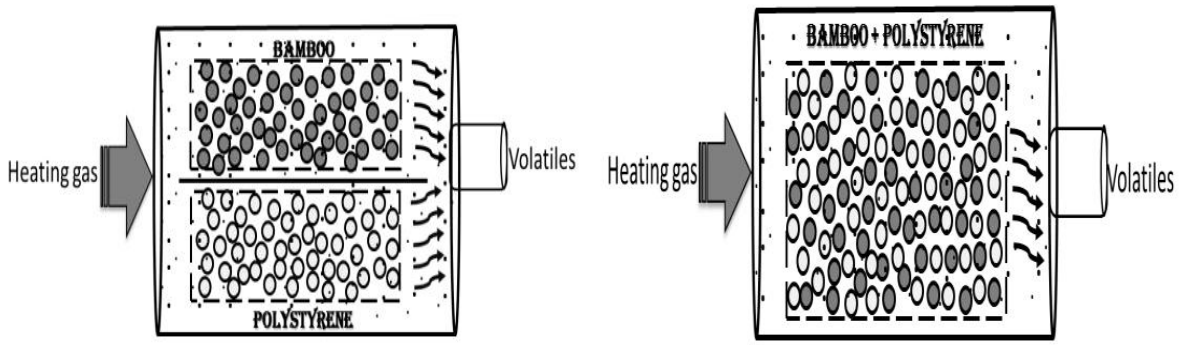

Figure 1: Reactor model illustration for the two different modelling approaches.

The following assumptions were made when constructing the model:

1. The shape of the pyrolysis particle is spherical.
2. Conduction is the only mode of heat transfer within the particle.
3. The volatiles leaving the particle do not interfere directly with the pyrolysis gas.
4. The only form of inter-particle interaction is heat transfer.

Reaction Kinetics:

We assume three primary reaction pathways:

1. Biomass decomposition:
   Biomass $\xrightarrow{k_1}$ Volatile (B) + Char (C) + Gas (G).
2. Plastics decomposition:
   Plastics $\xrightarrow{k_2}$ Volatile Hydrocarbon (P) + Gas (G).
3. Synergistic reactions:
   Volatile (B) + Volatile Hydrocarbon (P) $\xrightarrow{k_3}$ Enhanced Volatiles (S).

The reaction rates are modelled using Arrhenius kinetics:

$$k_i = A_i \exp\left(-\frac{E}{RT}\right) \tag{1}$$

Energy Balance:

The energy balance accounts for heat supplied, consumed and transferred in the reactor and is given as (Oyedun *et al.*, 2013):

$$\rho_{mixed} c_{p\,overall} \frac{\partial T}{\partial t'} = k_{mixed} \frac{1}{r'^2} \frac{\partial}{\partial r'}\left(r'^2 \frac{\partial T}{\partial r'}\right) + U^* A\left(T_w - T\right) + \Delta H_B A_B C_B e^{-\frac{E_B}{RT}} + \Delta H_P A_P C_P e^{-\frac{E_P}{RT}} \tag{2}$$

The initial and boundary conditions is formulated as:

$$T(r',0) = T_b, \quad \left.\frac{\partial T}{\partial r'}\right|_{r'=0} = 0, \quad -k^* \left.\frac{\partial T}{\partial r'}\right|_{r'=R} = h_T\left(T\big|_{r'=R} - T_b\right) \tag{3}$$

The density of the mixture is represented by (Feinstein, 1972):

$$\rho_{mixed} = \frac{1}{\left(\frac{x_B}{\rho_B}\right) + \left(\frac{x_P}{\rho_P}\right)} \tag{4}$$

The thermal conductivity of the mixture is represented by conductivity-mixture rule (Kasap and Capper, 2006):

$$k_{mixed} = x_B k_B + x_P k_P \tag{5}$$

The specific heat capacity of the mixed-feed is represented by (Gunther & Steimle, 1997):

$$c_{p\,overall} = x_B c_{pB} + x_P c_{pP} \tag{6}$$

where

A_i is pre-exponential factor $\left(s^{-1}\right)$, E_i is activation energy $\left(J/mol\right)$, R is universal gas constant $\left(8.314\ J/mol\right)$, T is absolute temperature $\left(K\right)$, ρ is density of feedstock $\left(kg/m^3\right)$, t' is reaction time $\left(s\right)$, k is thermal conductivity $\left(W/m\cdot K\right)$, c_p is specific heat capacity, C is concentration, ΔH is heat of reaction $\left(J/kg\right)$, r' is radius of a discrete layer $\left(m\right)$, x is blend ratio $\left(wt\ \%\right)$, h_T is convective heat transfer coefficient $\left(W/m^2\cdot K\right)$, $T\big|_{r'=R}$ is particle surface temperature $\left(K\right)$, T_b is bulk temperature $\left(K\right)$, U^* is the heat transfer coefficient, A is the surface area, T_w is wall temperature, ***Subscript***: B is Biomass (Bamboo), P is Plastics (Polystyrene), $mixed$ is mixed-particle, w is wall, b is bulk.

Method of Solution

Dimension Analysis

Substituting equations (4) – (6) into equations (2) and (3) and introducing dimensionless variables given as:

$$\left.\begin{array}{llll} r=\dfrac{r'}{R}, & t=\dfrac{U_0 t'}{R}, & f=\dfrac{E_P}{E_B}, & \psi=\dfrac{C_P}{C_{P0}}, \\ \phi=\dfrac{C_B}{C_{B0}}, & \theta=\dfrac{\left(T-T_b\right)}{\in T_b}, & \in=\dfrac{RT_b}{E_B}, & \end{array}\right\}, \tag{7}$$

where ψ, ϕ, θ and $\in$ are the dimensionless velocity, plastics concentration, bamboo concentration, temperature and activation energy parameter, respectively.

The system of governing equations (2) and (3), become

$$\frac{\partial\theta}{\partial t}=A\frac{1}{r^2}\frac{\partial}{\partial r}\left(r^2\frac{\partial\theta}{\partial r}\right)+B\left(h-\theta\right)+C\phi e^{\frac{\theta}{1+\in\theta}}+D\psi e^{\frac{f\theta}{1+\in\theta}} \tag{8}$$

$$\left.\theta\left(r,0\right)=0, \quad \left.\frac{\partial\theta}{\partial r}\right|_{r=0}=0, \quad \left.\frac{\partial\theta}{\partial r}\right|_{r=1}+Nu\theta\big|_{r=1}=0\right\}, \tag{9}$$

where

$a=\dfrac{x_P c_{pP}}{x_B c_{pB}}$, $b=\dfrac{\rho_B}{\rho_P}$, $c=\dfrac{1}{x_B\left(1+a\right)}$, $d=\dfrac{1}{x_P\left(1+\dfrac{1}{a}\right)}$, $\dfrac{1}{P_{e1}}=\dfrac{k_B}{\rho_B c_{pB} UR}$ is the Peclet energy number for Biomass, $\dfrac{1}{P_{e2}}=\dfrac{k_P}{\rho_P c_{pP} UR}$ is the Peclet energy number for Plastics, $q_1=\dfrac{U^* AR}{\rho_B c_{pB} U}$ is the heat source/sink for Biomas, $q_2=\dfrac{U^* AR}{\rho_P c_{pP} U}$ is the heat source/sink for Plastics, $h=\dfrac{\left(T_w-T_b\right)}{\in T_b}$, $\delta_1=\dfrac{\Delta H_B A_B RC_{B0} e^{-\frac{E_B}{RT_b}}}{\rho_B c_{pB} U\in T_b}$ is the Frank-Kamenetskii number for Biomass, $\delta_2=\dfrac{\Delta H_B A_B RC_{B0} e^{-\frac{E_B}{RT_b}}}{\rho_P c_{pP} U\in T_b}$ is the Frank-Kamenetskii number for Biomass, $\delta_3=\dfrac{\Delta H_P A_P RC_{P0} e^{-\frac{f E_B}{RT_b}}}{\rho_B c_{pB} U\in T_b}$ is the Frank-Kamenetskii number for Plastics, $\delta_4=\dfrac{\Delta H_P A_P RC_{P0} e^{-\frac{f E_B}{RT_b}}}{\rho_P c_{pP} U\in T_b}$ is the Frank-Kamenetskii number for Plastics, $Nu=\dfrac{h_T R}{k^*}$ is the Nusselt number, $A=\left(cx_B\left(x_B+bx_P\right)\dfrac{1}{P_{e1}}+dx_P\left(\dfrac{x_B}{b}+x_P\right)\dfrac{1}{P_{e2}}\right)$, $B=\left(cx_B q_1+dx_P q_2\right)$, $C=\left(cx_B\delta_1+dx_P\delta_2\right)$, $D=\left(cx_B\delta_3+dx_P\delta_4\right)$.

Analytical Solution Via OGPAM

Let $\in\to 0$, so that we can take an approximation:

$$\exp\left(\frac{\theta}{1+\in\theta}\right)\approx 1+\theta+\ldots \tag{10}$$

$$\exp\left(\frac{f\theta}{1+\in\theta}\right)\approx 1+f\theta+\ldots \tag{11}$$

Then equations (8) and (9) become

$$\left.\begin{aligned}&\frac{\partial\theta}{\partial t}=A\frac{1}{r^2}\frac{\partial}{\partial r}\left(r^2\frac{\partial\theta}{\partial r}\right)+E+F\theta\\ &\theta(r,0)=0,\qquad \left.\frac{\partial\theta}{\partial r}\right|_{r=0}=0,\qquad \left.\frac{\partial\theta}{\partial r}\right|_{r=1}+Nu\theta|_{r=1}=0\end{aligned}\right\} \tag{12}$$

where $E=(Bh+C\phi+D\psi)$, $\quad F=(C\phi+Df\psi-B)$

Here, equation (12) is solved using Olayiwola's generalised polynomial approximation method (OGPAM) (Olayiwola, 2022; Olayiwola *et al*. 2022a; Olayiwola *et al*., 2022b).

Compare equation (12) with the OGPAM equations (13) – (15) below:

$$\frac{\partial\phi}{\partial t}=\frac{k}{r^n}\frac{\partial}{\partial r}\left(r^n\frac{\partial\phi}{\partial r}\right)+F(r,t,\phi),\qquad t>0,\ \ r\in\Omega\ \ \left(\Omega\subset R^1,R^2 or\, R^3\right) \tag{13}$$

with the initial condition

$$\phi(r,0)=f(r) \tag{14}$$

and the boundary conditions

$$\alpha_1\left.\frac{\partial\phi}{\partial r}\right|_{r=a}+\beta_1\phi|_{r=a}=g_1(t),\qquad \alpha_2\left.\frac{\partial\phi}{\partial r}\right|_{r=b}+\beta_2\phi|_{r=b}=g_2(t) \tag{15}$$

We have

$k=A,\ \ n=2,\ \ \phi=\theta,\ F(r,t,\phi)=E+F\theta,\ f(r)=0,\ \ \alpha_1=1,\ \ \beta_1=0,\ \ g_1(t)=0,\ \alpha_2=1,\beta_2=Nu,$
$g_2(t)=0,\ \ a=0,\ \ b=1.$

Then

$$A_\theta=\left(1+\frac{Nu}{5}\right),\qquad B_\theta=-\frac{1}{20},\qquad C_\theta=\frac{1}{5} \tag{16}$$

Assume Olayiwola's generalized polynomial solution:

$$\theta(r,t)=\left(1+\frac{Nu}{2}\right)\theta|_{r=1}-\frac{Nu}{2}\theta|_{r=1}r^2 \tag{17}$$

Then

$$\begin{aligned}\frac{n+1}{b^{n+1}-a^{n+1}}\int_a^b r^nF(r,t,\phi)dr&=3\int_0^1 r^2\left(E+F\left(\left(1+\frac{Nu}{2}\right)\theta|_{r=1}-\frac{Nu}{2}\theta|_{r=1}r^2\right)\right)dr\\ &=3\int_0^1\left(\left(E+F\left(1+\frac{Nu}{2}\right)\theta|_{r=1}\right)r^2-F\frac{Nu}{2}\theta|_{r=1}r^4\right)dr\\ &=\left(E+F\left(1+\frac{Nu}{2}\right)\theta|_{r=1}\right)-\frac{3}{5}F\frac{Nu}{2}\theta|_{r=1}\\ &=E+F\left(1+\frac{Nu}{5}\right)\theta|_{r=1}\end{aligned} \tag{18}$$

That is

$$p_1(t)=F\left(1+\frac{Nu}{5}\right)\qquad \text{and} \qquad q_1(t)=E\,.$$

So,

$$p(t)=\frac{1}{\left(1+\frac{Nu}{5}\right)}\left(3ANu-F\left(1+\frac{Nu}{5}\right)\right)=\left(\frac{3ANu}{\left(1+\frac{Nu}{5}\right)}-F\right)=c_0\ \ (say) \tag{19}$$

$$q(t)=\frac{1}{\left(1+\frac{Nu}{5}\right)}E=\frac{E}{\left(1+\frac{Nu}{5}\right)}=c_1\ \ (say) \tag{20}$$

Then

$$\theta\big|_{r=1}=e^{-c_0t}\int_0^t c_1e^{c_0x}dx+f(r)e^{-c_0t}=\frac{c_1}{c_0}e^{-c_0t}e^{c_0x}\Big|_0^t=\frac{c_1}{c_0}e^{-c_0t}\left(e^{c_0t}-1\right)=\frac{c_1}{c_0}\left(1-e^{-c_0t}\right) \tag{21}$$

Thus

$$\theta(r,t)=\left(1+\frac{Nu}{2}\right)\frac{c_1}{c_0}\left(1-e^{-c_0t}\right)-\frac{Nu}{2}\frac{c_1}{c_0}\left(1-e^{-c_0t}\right)r^2=\frac{c_1}{c_0}\left(1-e^{-c_0t}\right)\left(1+\frac{Nu}{2}\left(1-r^2\right)\right) \tag{22}$$

The computation was done on equation (22) using the computer symbolic algebraic package MAPLE 2021 version.

Results and Discussion

The simulation was carried out to show the impact of the model parameters by employing Olayiwola's Generalised Polynomial Approximation Method (OGPAM) on equations (8) and (9). We are concerned with the nature of the solutions obtained when (i) the two feedstocks (Bamboo and Polystyrene) are pyrolysed at the same time at a pre-defined ratio. (ii) the samples were mixed in a pre-defined ratio of 1:3, 1:1 and 3:1 (25% PS: 75% Bamboo, 50% PS: 50% Bamboo and 75%PS: 25% Bamboo). The computation of equations (22) was done using the MAPLE 2021 version.

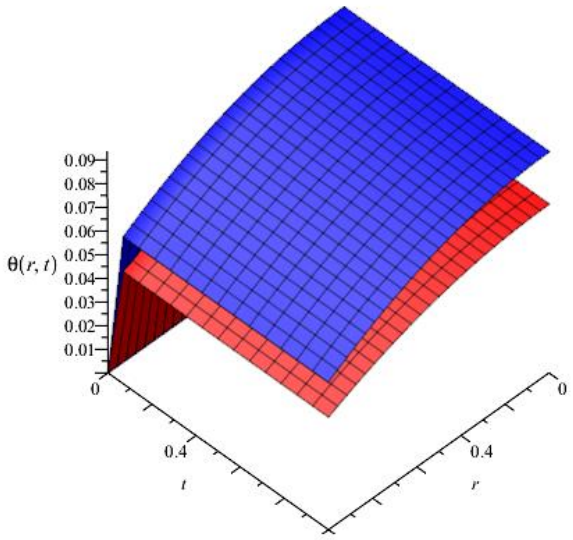

.....Bamboo .....Polystyrene

Figure 1: Temperature history at $x_B=100\%,\ x_P=100\%$ ***for*** $N_u=1,\ P_{e1}=0.3,\ P_{e2}=0.4$**.**

Figure 1 shows the temperature history when the two feedstocks (Bamboo and Polystyrene) are pyrolysed at the same time at a pre-defined ratio of 1:1. After the sudden temperature rise, the graph displays a rapid transition to a steady solution. This graph revealed that the

energy required at the early stage of polystyrene pyrolysis is much higher than that of biomass pyrolysis.

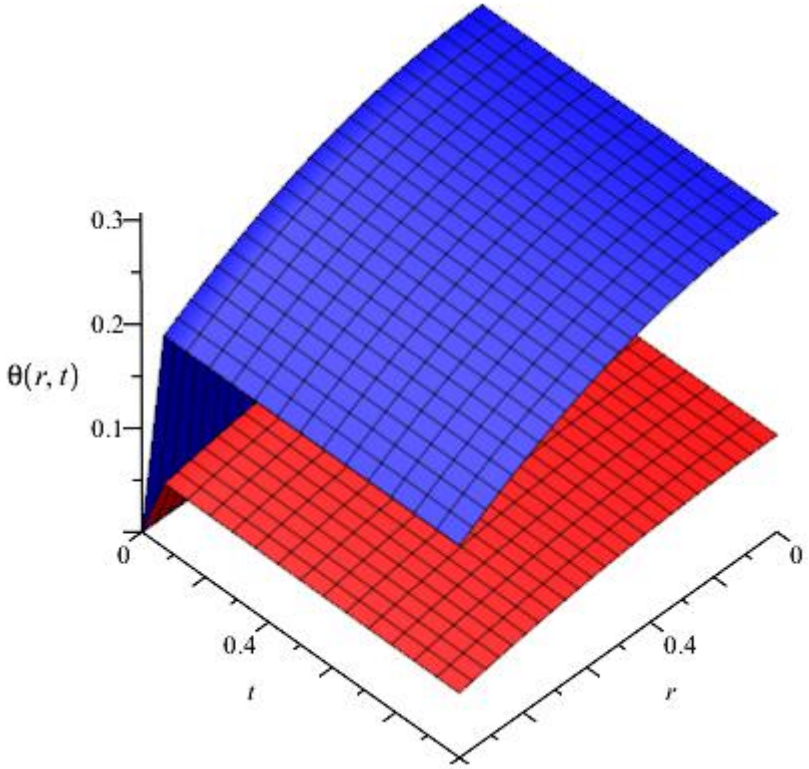

..... 75% Bamboo ..... 25% Polystyrene

Figure 2: Temperature history at $x_B = 75\%, x_P = 25\%$ ***for*** $N_u = 1, P_{e1} = 0.3, P_{e2} = 0.4$ ***.***

Figure 2 shows the temperature history when the two feedstocks (Bamboo and Polystyrene) are pyrolysed at the same time at a pre-defined ratio of 3:1. After the sudden temperature rise, the graph displays a rapid transition to a steady solution. This graph revealed that the energy required at the early stage of polystyrene pyrolysis is much higher than that of biomass pyrolysis.

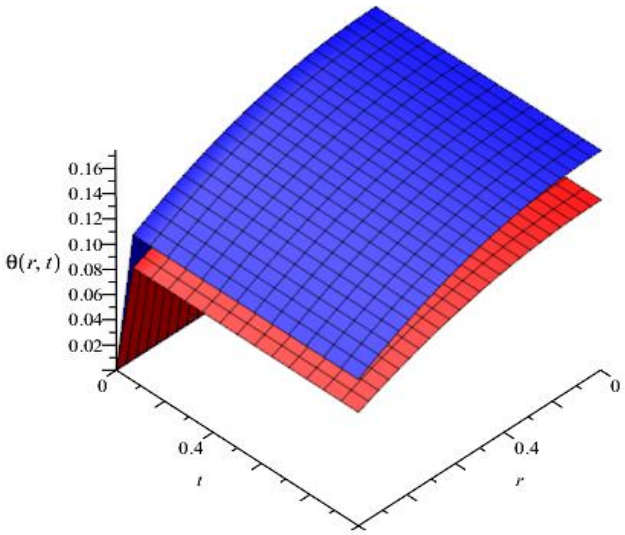

..... 50% Bamboo ..... 50% Polystyrene

Figure 3: Temperature history at $x_B = 50\%,\ x_P = 50\%$ ***for*** $N_u = 1,\ P_{e1} = 0.3,\ P_{e2} = 0.4$.

Figure 3 shows the temperature history when the two feedstocks (Bamboo and Polystyrene) are pyrolysed at the same time at a pre-defined ratio of 1:1. After the sudden temperature rise, the graph displays a rapid transition to a steady solution. This graph revealed that the energy required at the early stage of polystyrene pyrolysis is much higher than that of biomass pyrolysis.

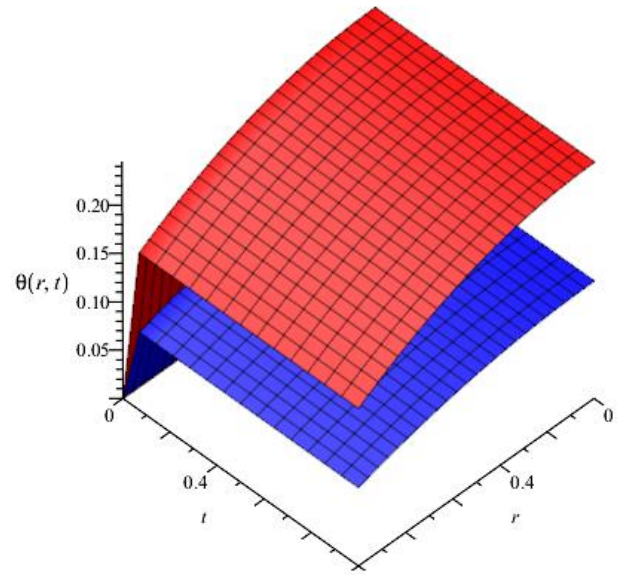

..... 25% Bamboo ..... 75% Polystyrene

Figure 4: Temperature history at $x_B = 25\%,\ x_P = 75\%$ ***for*** $N_u = 1,\ P_{e1} = 0.3,\ P_{e2} = 0.4$.

Figure 4 shows the temperature history when the two feedstocks (Bamboo and Polystyrene) are pyrolysed at the same time at a pre-defined ratio of 1:1. After the sudden temperature rise, the graph displays a rapid transition to a steady solution. This graph revealed that the energy required at the early stage of polystyrene pyrolysis is much higher than that of biomass pyrolysis.

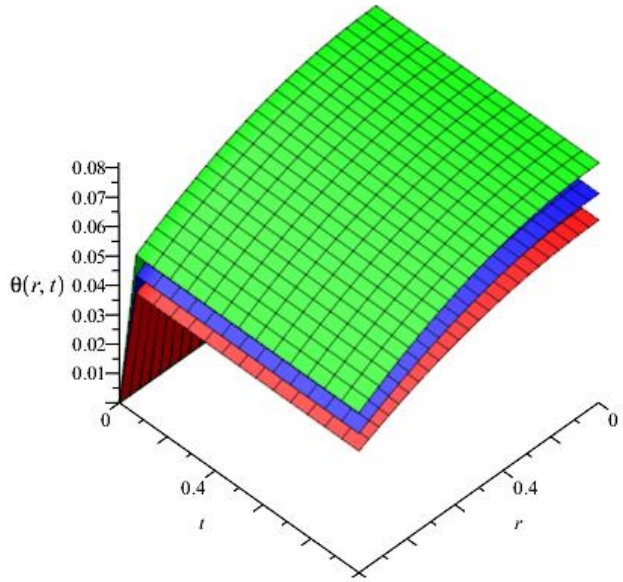

... 75% Bamboo 25% Polystyrene ... 25% Bamboo 75% Polystyrene ... 50% Bamboo 50% Polystyrene

Figure 5: Temperature history at *25% PS: 75% Bamboo, 50% PS: 50% Bamboo and 75%PS: 25% Bamboo* ***for*** $N_u = 1,\ P_{e1} = 0.3,\ P_{e2} = 0.4$ ***.***

Figure 5 shows the temperature history when the samples were mixed in a pre-defined ratio of 1:3, 1:1 and 3:1 (25% PS: 75% Bamboo, 50% PS: 50% Bamboo and 75%PS: 25% Bamboo). After the sudden temperature rise, the graph displays a rapid transition to a steady solution. This graph revealed that the energy required at the early stage of co-pyrolysis is much higher in a pre-defined ratio of 1:1 follow by a pre-defined ratio of 1:3.

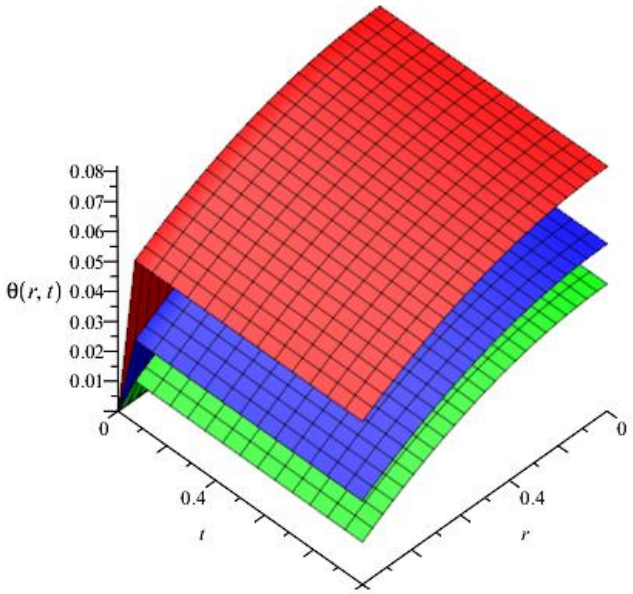

Figure 6: Temperature history at $N_u = 1,\ N_u = 2,\ N_u = 3$ ***for*** $P_{e1} = 0.3,\ P_{e2} = 0.4$ ***.***

Figure 6 shows the temperature history when the samples were mixed in a pre-defined ratio of 1:1 (50% PS: 50% Bamboo) for various values of Nusselt Number. After the sudden temperature rise, the graph displays a rapid transition to a steady solution with time. This graph revealed that temperature decreases as the Nusselt number increases.

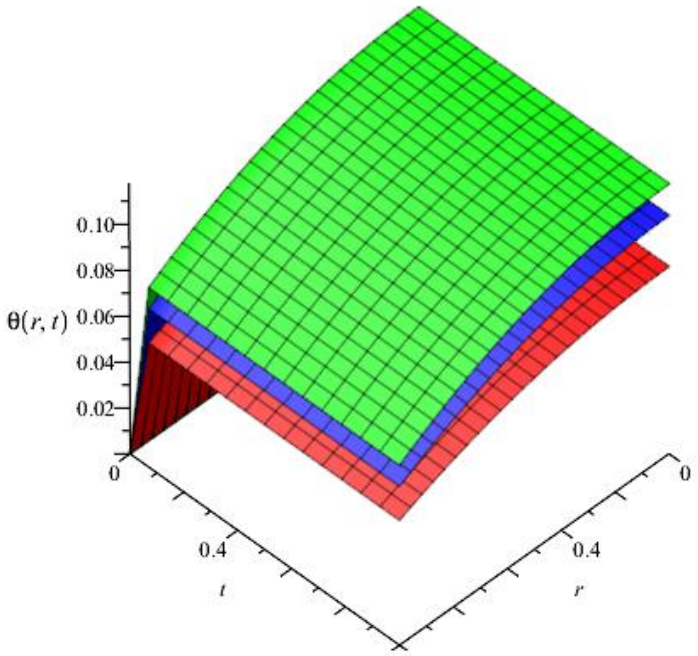

Figure 7: Temperature history at $P_{e1} = 0.3,\ P_{e1} = 0.5,\ P_{e1} = 0.7$ ***for*** $N_u = 1,\ P_{e2} = 0.4$ ***.***

Figure 7 shows the temperature history when the samples were mixed in a pre-defined ratio of 1:1 (50% PS: 50% Bamboo) for various values of Peclet Number for Bamboo. After the sudden temperature rise, the graph displays a rapid transition to a steady solution with time. This graph revealed that temperature increases as the Peclet Number for Bamboo increases.

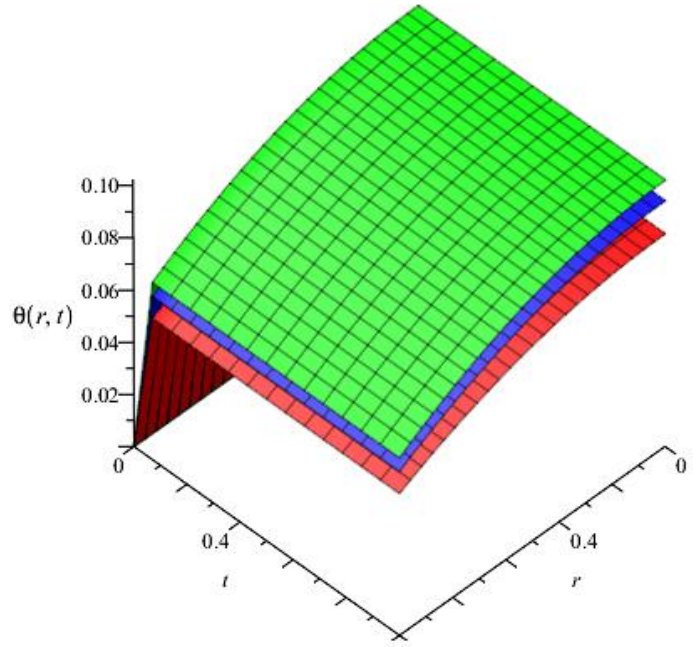

Figure 8: Temperature history at $P_{e2} = 0.4,\ P_{e2} = 0.6,\ P_{e2} = 0.8$ ***for*** $N_u = 1,\ P_{e1} = 0.3$ ***.***

Figure 8 shows the temperature history when the samples were mixed in a pre-defined ratio of 1:1 (50% PS: 50% Bamboo) for various values of Peclet Number for Polystyrene. After the sudden temperature rise, the graph displays a rapid transition to a steady solution with time.

This graph revealed that temperature increases as the Peclet Number for Polystyrene increases.

Conclusion

A co-pyrolysis modelling approach is proposed and evaluated in this study. Two different modelling approaches were used to evaluate the possible synergistic effect in terms of energy usage between plastics (PS) and biomass (bamboo) as a case study. An approximate analytical solution is provided for the model formulated. There is a distinct difference in the heat flow profile for plastics and biomass feedstocks. The result of the energy usage shows a reduction in energy for the mixed blends for the two approaches. Approach two, which allows interaction between the two feedstocks, has a greater reduction in overall energy up to 79% when the ratio of the PS feed was 25 %.

The simulation results revealed the impact of the model parameters, and the following conclusion can be drawn:

1. A reduction in the Nusselt number enhanced the temperature in the reactor.
2. An increase in the Peclet numbers of Bamboo enhanced the temperature in the reactor.
3. An increase in the Peclet numbers of Polystyrene enhanced the temperature in the reactor.

Conflict of Interest: The authors declared that no conflict of interest may arise from the publication.

References

Feinstein, H. I. (1972). Density of a binary mixture. A classroom or laboratory exercise. *Journal of Chemical Education*, 49, 111.

Gao, X., Liu, Y., & Chen, H. (2022). Machine learning models for predicting product distribution in biomass pyrolysis. *Renewable Energy, 180*, 1023-1035.

Günther, D., & Steimle, F. (1997). Mixing rules for the specific heat capacities of several HFC-mixtures. *International Journal of Refrigeration*, 20, 235-243.

Kasap, S., & Capper, P. (2006). *Springer handbook of electronic and photonic materials.* Springer.

Li, J., Zhang, T., & Wang, Y. (2019). Synergistic effects of biomass and plastic co-pyrolysis: A review. *Energy Conversion and Management, 198*, 111780.

Olayiwola, R. O. (2022). Solving parabolic equations by Olayiwola's generalized polynomial approximation method. *International Journal of Mathematical Analysis and Modelling*, 5(3), 24 - 43.

Olayiwola, R. O., Mohammed, I. B. S., Oyubu, J. P., Abdullahi, U. A., Anyanwu, E. O., Abubakar, A. D., & Yisa, E. M. (2022a). Tracking oscillating edge-flames: A mathematical approach. *International Journal of Mathematical Analysis and Modelling*, 5(4), 58 – 71.

Olayiwola, R. O., Yusuf, S. I., Abubakar, A. D., Audu, K. J., Mohammed, I. B. S., Anyanwu, E. O., Abdullahi, U. A., & Oyubu, J. P. (2022b). Thermal explosion with convection in

porous media: a mathematical approach. *International Journal of Mathematical Analysis and Modelling*, 5(4), 95 – 108.

Oyedun, A. O., Gebreegziabher, T., & Hui, C. W. (2013). Co-pyrolysis of biomass and plastics waste: A modelling approach. *Chemical Engineering Transactions*, 35, 883-888 DOI:10.3303/CET1335147

Sharma, R., Kumar, S., & Singh, R. (2021). Advances in co-pyrolysis of biomass and plastics: Reaction mechanisms and product characterization. *Bioresource Technology, 327*, 124787.

Singh, P., Verma, R., & Patel, R. (2020). Computational fluid dynamics (CFD) modeling of biomass pyrolysis reactors: Challenges and opportunities. *Chemical Engineering Science, 224*, 115837.

Wang, H., He, Y., & Zhou, Z. (2020). Bio-oil quality improvement via co-pyrolysis of biomass and plastics: A review. *Fuel, 265*, 116947.

Xie, J., Sun, W., & Guo, Y. (2021). Kinetic modeling of biomass pyrolysis: An integrated Arrhenius and DAEM approach. *Energy, 214*, 118873.

Zhang, C., Feng, L., & Yu, H. (2019). Distributed Activation Energy Model (DAEM) for predicting co-pyrolysis kinetics of mixed waste feedstocks. *Journal of Thermal Analysis and Calorimetry, 136*, 987-996.